NANO · MICRO small
www.small-journal.com

"Non-Naked" Gold with Glucose Oxidase-Like Activity: A Nanozyme for Tandem Catalysis

Haijiao Zhang, Xin Liang, Lei Han, and Feng Li**

It has been widely reported that "naked" gold nanoparticles (Au NPs) without protectors have glucose oxidase (GOx)-like activity, and the use of protectors can inhibit the GOx-like activity. Here, "non-naked" Au NPs with GOx-like activity are synthesized by using protein as protector. Although "naked" Au NPs have peroxidase-like activity and GOx-like activity, the optimal pH ranges of the both activities are obviously different. Fortunately, as-synthesized "non-naked" Au NPs show the dual enzyme-like activities at the same pH. So, "non-naked" Au NPs can be described as "tandem nanozyme." As another bonus, the participation of protein protector can stabilize the GOx-like activity and make Au NPs modifiable. Even though Au NPs are connected with graphene oxide (GO), the GOx-like activity is still not changed. Further, Au NPs-GO nanocomposites are applied on the one-pot nonenzymatic glucose colorimetric detection. The "non-naked" gold not only broadens the species of tandem nanozymes, but also facilitates the functionalization of nanozymes, which is promising for immunoassay, biosensor, and medical treatment.

1. Introduction

With the development of nanotechnology, nanozymes are widely used as substitutes of natural enzymes.[1–4] The reported enzyme-like activities include the peroxidase-like activity,[5–9] superoxide dismutase-like activity,[10–12] catalase-like activity,[13–15] and so on. However, there are relatively few reports about glucose oxidase (GOx)-like activity.[2,16] In 2004, Rossi and co-workers first discovered that the "naked" gold nanoparticles (Au NPs) synthesized without protectors or stabilizers had GOx-like activity.[17] However, the GOx-like activity of "naked" Au NPs has short life due to the instability without stabilizer, and the use of stabilizer and protectors (such as polyvinyl alcohol, polypyrrolidone, and tetrahydroxymethylphosphonium chloride) can inhibit the GOx-like activity.[17,18] Since then, the GOx-like activity of Au NPs was extensively applied on various fields. For example, Fan and co-workers realized the detection of DNA by the Au NPs-catalyzed oxidation of glucose at the neutral pH.[19] Qu's group utilized the mesoporous silica as supporter to help the formation of small and well-dispersed Au NPs and stabilize the GOx-like activity.[20] Further, a one-pot glucose detection for more than 7 h incubation was developed, where GOx-like activity worked at pH 7.4, and then the product gluconic acid decreased the ambient pH to around 4.2 after about 7 h, and activated the peroxidase-like activity.[20] Fan's group synthesized Au NPs with GOx-like activity by using sodium citrate as the reductant.[21] Because Au NPs-catalyzed oxidation of glucose occurred in natural pH and natural horseradish peroxides (HRPs) could catalyze the chromogenic reaction at weakly acidic pH, the glucose detection was achieved by a two-step method.[21] It is worth noting that these reported GOx-mimicking Au NPs have some following disadvantages. (1) The surfaces of Au NPs lack modifiable groups and are hardly modified with some functional molecules, because of the absence of stabilizers or protectors in the synthesis process of Au NPs.[17] (2) Moreover, Au NPs can be easily poisoned by binding with sulfur compounds, making the functionalization of Au NPs more difficult.[17] (3) The previous reported Au NPs show GOx-like activity at neutral and alkalic pH,[22] but peroxidase-like activity at acidic pH, which fails to realize fast, enzyme-free, and one-pot glucose detection and will increase the cost of assay method.[20] (4) In general, the optimal pHs (acidic pH) of the peroxidase mimics and commercial horseradish peroxides were different from the GOx-like activity of these Au NPs,[9,23] resulting in the two-step operation for the glucose colorimetric detection.[21]

In this work, we discovered that Au NPs with natural protein (bovine serum albumin, BSA) as stabilizer and protector showed the GOx-like activities. Interestingly, "non-naked" Au nanoparticles (Au@BSA NPs) could simultaneously show GOx-like activity and peroxidase-like activity at the same pH, benefiting the establishment of one-pot enzyme-free glucose detection. Moreover, Au@BSA NPs possessed amino groups on the surface due to the participation of BSA, facilitating the covalent modification of other functional molecules onto the surface of Au NPs. So, Au@BSA NPs were covalently bonded with graphene oxide (GO) by the amide bond in order to confirm the above advantage of Au@BSA NPs. Further, one-pot enzyme-free strategy based on sole nanozyme (Au@BSA NPs) was developed for the fast colorimetric detection of glucose. The as-synthesized Au@BSA NPs not only broaden the species

H. Zhang, X. Liang, Prof. L. Han, Prof. F. Li
College of Chemistry and Pharmaceutical Sciences
Qingdao Agricultural University
700 Changcheng Road, Qingdao 266109, China
E-mail: hanlei@qau.edu.cn; lifeng@qau.edu.cn

The ORCID identification number(s) for the author(s) of this article can be found under https://doi.org/10.1002/smll.201803256.

DOI: 10.1002/smll.201803256

of nanozymes, but also have promising potential for application on the immunoassay and biomedical sensor based GOx mimics.

2. Results and Discussion

2.1. Morphology Characterization of Au@BSA NPs

Au@BSA NPs were synthesized by a bio-templated method (**Figure 1**a). First, chloroauric acid ($HAuCl_4$) mixed with different concentrations of BSA where BSA served as stabilizer. After the incubation for 1 h, the reductant sodium borohydride ($NaBH_4$) was added into the mixture to reduce $HAuCl_4$ to Au@BSA NPs. Then, their morphologies were observed by transmission electron microscope (TEM) (Figure 1b–e). Different diameters (12, 8, 2, and 4 nm) of Au@BSA NPs were, respectively, obtained by changing the concentration of BSA (1, 3, 6, and 10 μM), implying the effect of BSA concentration on the size of Au@BSA NPs (Figure S1, Supporting Information). In addition, each kind of NPs had good monodispersity.

In order to further study the surface charge properties of Au@BSA NPs, the zeta potentials of Au@BSA NPs with different sizes were detected. As shown in Figure 1f, all Au@BSA NPs were electronegative and the potentials of Au@BSA NPs slightly lowered with the increase of BSA concentration. So, Au@BSA NPs with 4 nm in diameter had highest negative potential. Further, Au@BSA NPs with the diameter of 4 nm were characterized by X-ray diffraction (XRD) assay (Figure 1g). The XRD pattern of Au@BSA NPs exhibited sharp diffraction peaks, which was completely consistent with the standard spectrogram of Au (JCPDS No. 04-0784), demonstrating high purity and good crystallinity of Au@BSA NPs.

2.2. Comparison of the Peroxidase-Like Activities of Different Au@BSA NPs

To verify the peroxidase-like activities of Au@BSA NPs with different sizes, the catalytic reactions with hydrogen peroxide (H_2O_2) and 3,3′,5,5′-tetramethylbenzidine (TMB) as the substrates were conducted, where TMB was oxidized by H_2O_2 to TMB*$^+$ in the present of the peroxidase mimetics. As shown in **Figure 2**a and Figure S2 (Supporting Information), the reaction solution with various Au@BSA NPs showed intense characteristic absorbance of TMB*$^+$, proving that all four kinds of Au@BSA NPs had intrinsic peroxidase-like activities. Furthermore, the different sizes of Au@BSA NPs showed different peroxidase-like activities and Au@BSA NPs with 4 nm in diameter showed the optimal activity, indicating that moderate size of Au@BSA NPs had better catalytic performance. To further demonstrate the above results, the time-dependent absorbances of reaction solutions were measured at 650 nm (Figure S3, Supporting Information). The reaction catalyzed by Au@BSA NPs with 4 nm in diameter had the optimal reaction rate, which was consistent with the spectroscopic data (Figure 2a). In addition, Au@BSA NPs were replaced by BSA in the above reaction and there was not observable activity (Figure S4, Supporting Information), testifying that the peroxidase-like activity came from Au NPs.

To further confirm the peroxidase-like activity of Au@BSA NPs, other chromogenic reagents 2,2′-azinobis(3-ethylbenzothiazoline-6-sulfonic acid ammonium salt) (ABTS) and o-phenylenediamine (OPD) were used as substrates to estimate the peroxidase-like activities of the NPs, and the solution in the absence of Au@BSA NPs showed obvious absorption peaks at 415 and 450 nm, respectively (Figure S5, Supporting Information), demonstrating the excellent peroxidase-like activities.

2.3. Discovery and Comparison of the GOx-Like Activities of Au@BSA NPs

To verify the GOx-like activities of Au@BSA NPs and compare the activities of Au@BSA NPs with different sizes, a two-step analytical approach was conducted. The reaction system containing Au@BSA NPs and glucose was incubated in air and then the product H_2O_2 was detected by the HRP-catalyzed oxidation of TMB. As shown in Figure 2b and Figure S6 (Supporting Information), there were obvious absorption peaks at 650 nm for the reaction solutions containing Au@BSA NPs, demonstrating that the first step of catalytic reaction indeed produced H_2O_2 and Au@BSA NPs had inherent GOx-like activities. Unlike peroxidase-like activities of Au@BSA NPs (Figure 2a), all reaction solutions showed almost the same absorption peak at 650 nm (Figure 2b), indicating all four kinds of Au@BSA NPs had similar activities. Smaller sizes (2–4 nm) showed slightly higher GOx-like activities.

Previous mechanism studies illuminated that the aerobic oxidation of glucose follows the Eley–Rideal mechanism where glucose is adsorbed on the surface of Au catalysts and then reacts with O_2.[24,25] Therefore, the reason why BSA showed nearly negligible effect on the GOx-like activity may be that the dosage of binding BSA was not enough to inhibit the accessibility of glucose. To verify the hypothesis, overdosage of BSA (30×10^{-6} M) was used in the synthesis of Au@BSA NPs and their GOx-like activities obviously declined (Figure S7, Supporting Information), demonstrating the Eley–Rideal mechanism. In contrast, "naked" Au NPs without BSA were also applied on the above reaction at pH 4.0 and the absorbance peak of reaction solutions was lower than these of Au@BSA NPs (Figure S7, Supporting Information), confirming the necessity of BSA.

Taken together, Au@BSA NPs had dual enzyme-mimicking activities (GOx-like and peroxidase-like activities), but the optimal diameters were different for the both activities. To further research the influence of sizes on reaction rate of cascade reaction based on dual enzyme-mimicking activities, the reaction system containing glucose, Au@BSA NPs, and TMB was performed. Because the initial reaction solution lacked H_2O_2, the peroxidase-mimicking catalytic reaction would only be started by H_2O_2 generated from GOx-mimicking catalytic reaction. As shown in Figure 2c, for all sizes of Au@BSA NPs, the absorbance of all solution gradually increased over time, confirming Au@BSA NPs had the GOx-like activity. Moreover, the reaction rate was relied on the sizes of Au@BSA NPs and the diameter of 4 nm had the maximum activity. To further prove the above result, the absorbances of reaction solutions were detected and Au@BSA NPs with the diameter of 4 nm showed the maximal catalytic activity (Figure 2c) and highest absorption

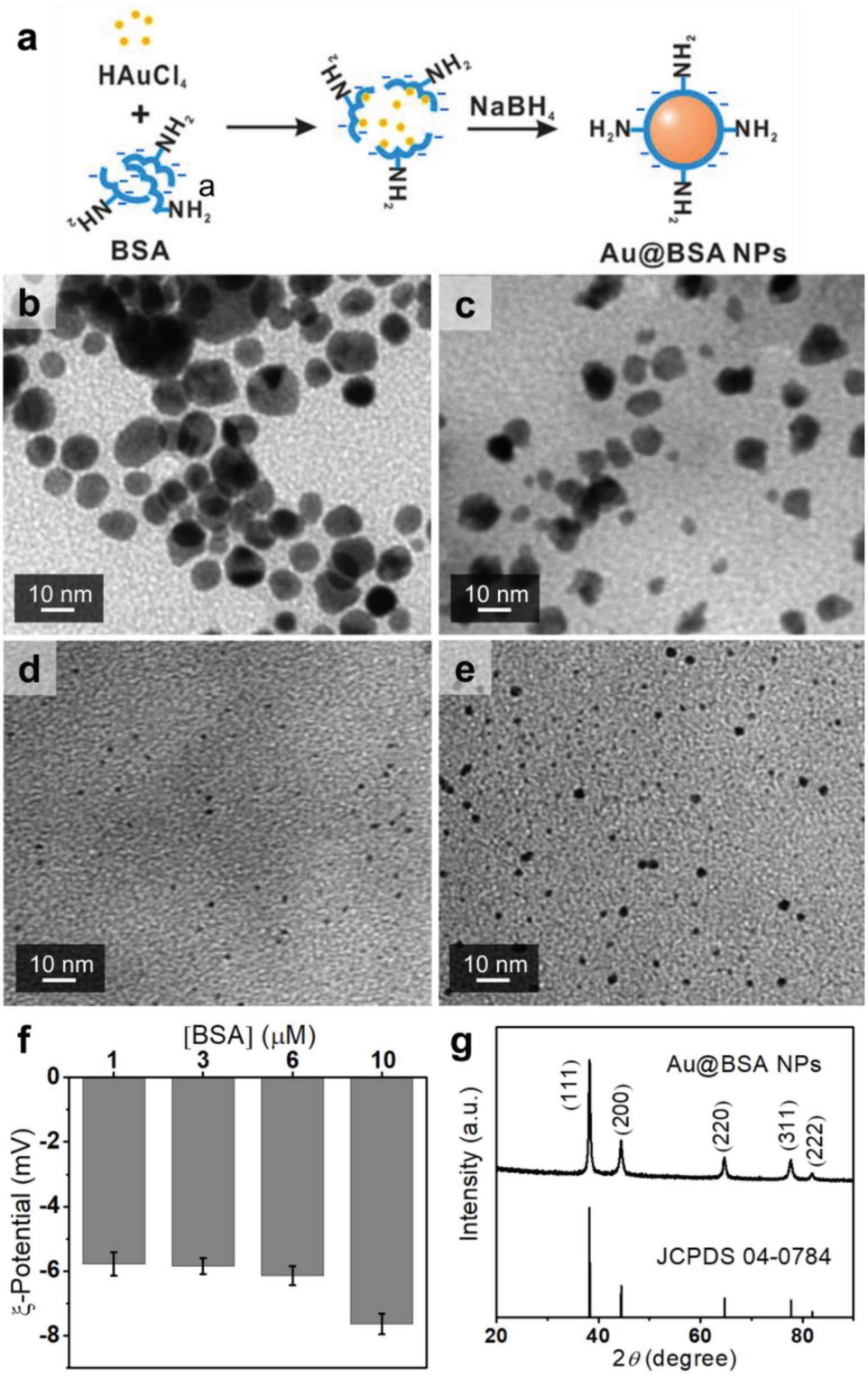

Figure 1. BSA-directed synthesis and characterization of Au@BSA NPs. a) Synthesis schematic of Au@BSA NPs. b–e) TEM images of Au@BSA NPs with the different dosages of BSA [(b) 1 μM; (c) 3 μM; (d) 6 μM; (e) 10 μM] in $HAuCl_4$ solution (5×10^{-3} M). f) The zeta potentials of Au@BSA NPs with the different dosages of BSA. g) XRD patterns of Au@BSA NPs with BSA (10 μM) and the standard values of Au (JCPDS No. 04-0784). The diffraction peaks corresponding to (110), (200), (220), (311), and (222) crystal plants were at 2θ values of 38.26°, 44.42°, 64.74°, 77.74°, and 81.88°, respectively.

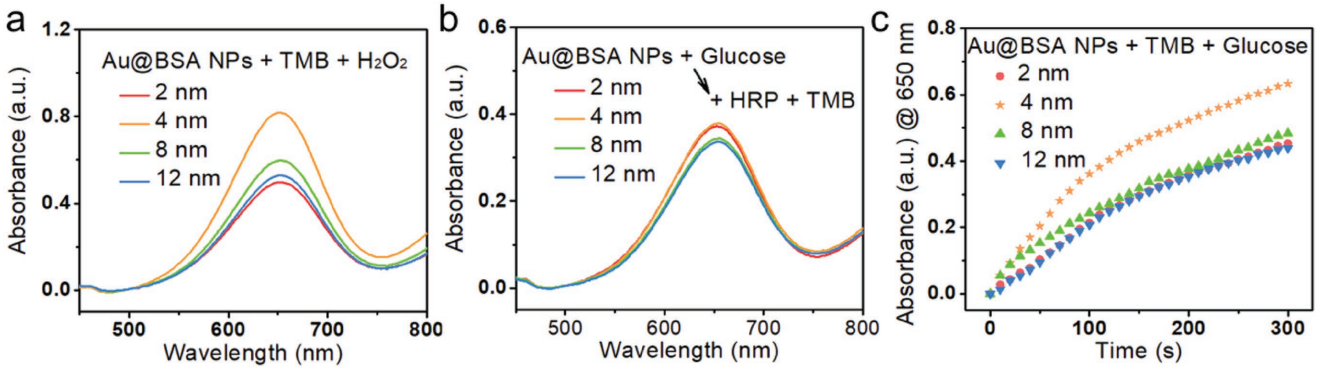

Figure 2. The dual enzyme-like activities of Au@BSA NPs with different diameters. a) Absorbance curves for the peroxidase-like activity. b) Absorbance curves for the GOx-like activity. c) Time-dependent absorbance for the one-pot reaction based on dual enzyme-like activities.

peak (Figure S8, Supporting Information). Therefore, the GOx-like activity of Au@BSA NPs was verified by the multiple verification strategies. This was an exciting discovery. According to the previous report, "non-naked" Au NPs with the protector did not have GOx-like activity. Here, the "non-naked" Au NPs with BSA as protector showed remarkable GOx-like activity.

2.4. pH Optimization of Tandem Enzyme-Like Activities

To further characterize the peroxidase-like and GOx-like activities of Au@BSA NPs, we studied the effect of pH on dual enzyme-like activities. For the peroxidase-like activities (**Figure 3**a), Au@BSA NPs showed peroxidase-like activity at weakly acidic pH and remained more than 90% maximum activity in pH range from 3.5 to 4.5. On the other hand, for the GOx-like activities, Au@BSA NPs exhibited GOx-like activities at wide pH range and remained more than 90% maximum activity in pH 3.0–6.0. Even if pH was 7.0, Au@BSA NPs remained above 80% relatively activity. According to the above results, the peroxidase-like and GOx-like activities of Au@BSA NPs have overlapped optimal pH range (optimal pH range was defined as the pH range in which catalytic activity remained more than 90% maximum activity).

In previous literatures, the optimal pH ranges of GOx-like activities and the peroxidase-like activities of Au NPs were generally different in order that these Au NPs only had one kind of enzyme-mimicking activity at a certain pH. By contrast, we had successfully synthetized a unique nanozyme (Au@BSA NPs), which had the similar pH range of dual enzyme activities. So, as-synthesized Au@BSA NPs could be called as "tandem nanozyme," which had two catalytic activities (peroxidase-like and the GOx-like activities) and could simultaneously catalyze the cascade reactions.[2]

In order to further optimize the pH of tandem enzyme-like activity, the one-pot reaction was conducted. As shown in Figure 3b, the NPs exhibited optimal activities at pH 4.0, implying that the both optimum pH ranges of the peroxidase-like and the GOx-like activities were partially overlapped. This was consistent with the above conclusions. Therefore, Au@BSA NPs can be served as a tandem nanozyme, which would be beneficial to apply to one-pot nonenzyme glucose detection.

As controls, Au@lysozyme NPs and Au@citrate NPs were also synthesized and applied on the one-pot reaction (Figure S9, Supporting Information). The unobservable absorption peaks demonstrated that Au@lysozyme NPs, Au@citrate NPs could not simultaneously show dual enzyme-like

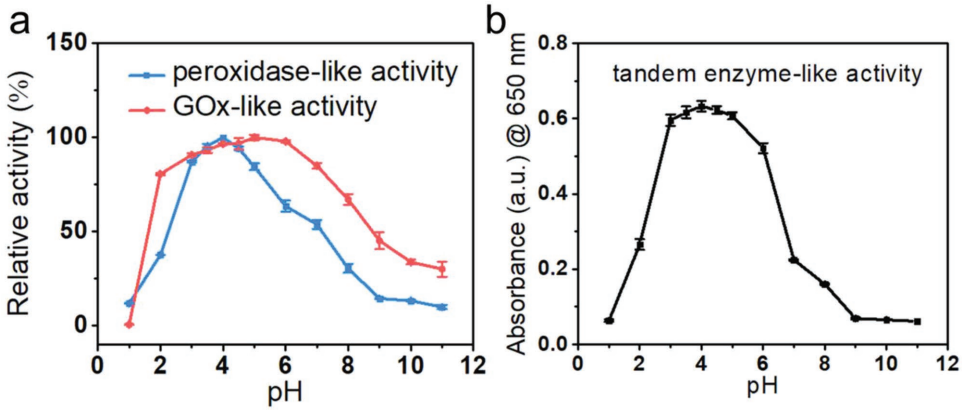

Figure 3. pH optimization of dual enzyme-like activities. a) The optimization of pH for the peroxidase-like and GOx-like activities of Au@BSA NPs. The highest point was defined as 100% of relative activity. b) The tandem enzyme activities of Au@BSA NPs.

activities at pH 4.0, implying the important role of BSA for the tandem enzyme-like activity.

2.5. Modifiable Au@BSA NPs

As another advantage, Au@BSA NPs can be facilely functionalized because of BSA as protector. In previous reports, to avoid the loss of the GOx-like activity, protector was not employed for the synthesis of Au NPs. So, these Au NPs had no functional groups on their surfaces and the further modification could inhibit the GOx-like activity. On the contrary, Au@BSA NPs were synthesized by using BSA as protector and stabilizer, and had amino group and carboxyl group on their surfaces, facilitating the further modification.

To verify the above advantages of Au@BSA NPs, GO (Figure S10, Supporting Information) was used as the model supporter for the covalent modification of Au@BSA NPs (**Figure 4**a). The carboxyl group of GO can be activated by 1-ethyl-3-(3-dimethylaminopropyl) carbodiimide hydrochloride (EDC) and *N*-hydroxysuccinimide (NHS), and then covalently bonded with Au@BSA NPs by an amide reaction between the carboxyl group of GO and the amino group of Au@BSA NPs (Figure 4a). TEM image of Au@BSA-GO nanocomposites showed that Au@BSA NPs uniformly dispersed on GO (Figure 4b). Subsequently, the GOx-like activities of Au@BSA NPs and Au@BSA NPs-GO nanocomposites were investigated and compared (Figure 4c). Excitingly, Au@BSA NPs and Au@BSA NPs-GO nanocomposites had similarity activities, indicating that the surface modification of Au@BSA NPs could not affect their GOx-like activity. The above results were clearly different from previously reported GOx-like Au NPs, which not only lacked modifiable groups but also were easily be inactivated by protector and molecular modification. In this contribution, the groups on the surface of GOx-like nanozymes would facilitate the functionalization of nanozymes with some molecules, such as antibody, enzyme, and fluorescence probe, which are promising for immunoassay, biosensor, and medical treatment.

Diabetes mellitus is a major public health problem,[26] which can directly affect the daily life and the health of people. So far, many methods have been explored for the detection of glucose, such as fluorometry,[27] spectrophotometry,[28] chromatography,[29] and electroanalysis.[30] Thereinto, as a common and commercial method, spectrophotometry has been widely used for clinical detection, where GOx and peroxidase are generally used as the catalysts of the colorimetric reaction.[31] Based on the dual enzyme-like activities of Au@BSA-GO nanocomposites, we built a one-pot enzyme-free strategy for colorimetric assay of glucose, where the oxidation of glucose and the

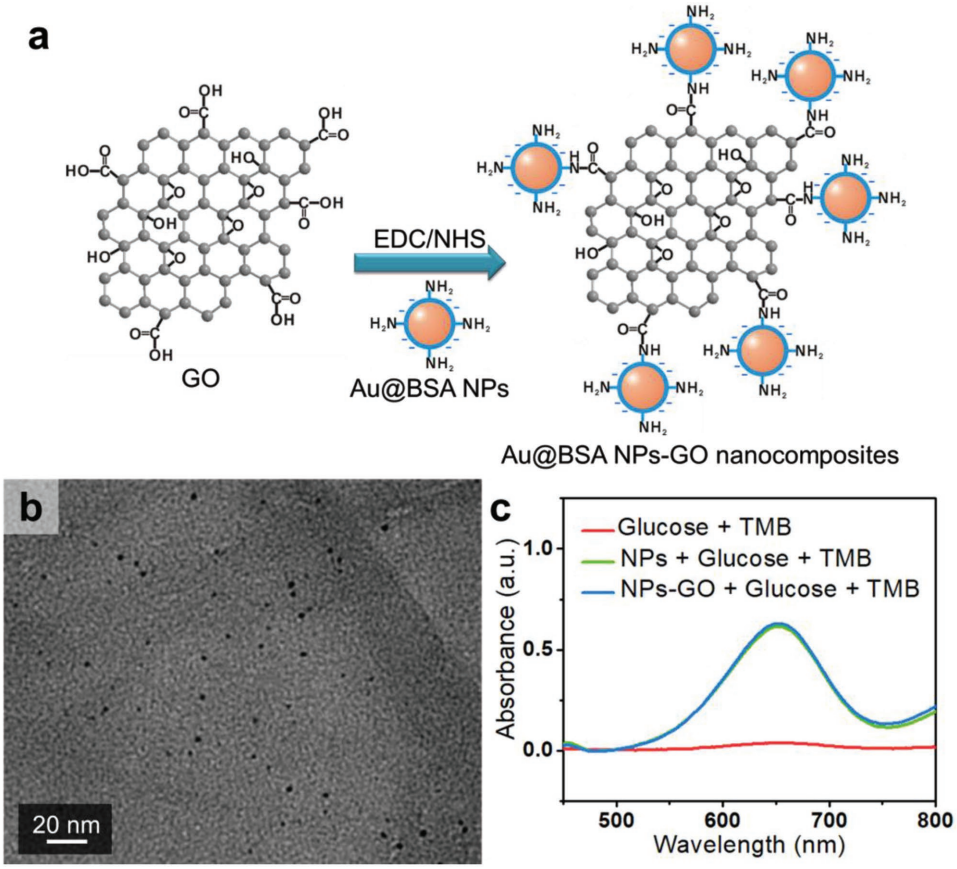

Figure 4. Synthesis and characterization of Au@BSA-GO nanocomposites. a) Synthesis schematic of Au@BSA-GO nanocomposites. b) TEM image of Au@BSA-GO nanocomposites. c) Absorbance curves of TMB oxidation catalyzed by Au@BSA-GO nanocomposites and controls for 5 min in acetate buffer (100×10^{-3} M, pH 4.0) with glucose.

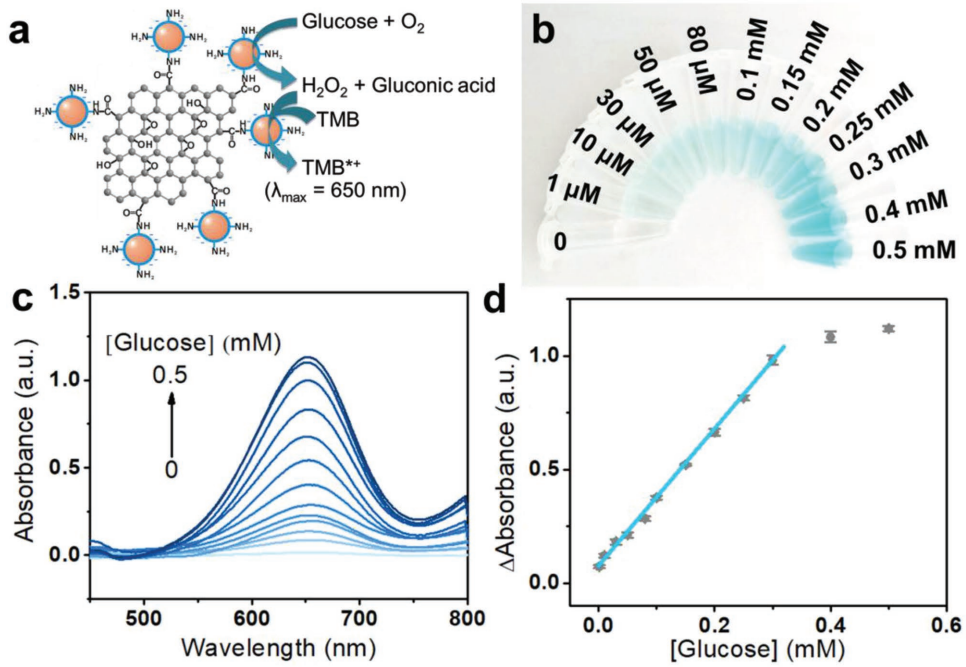

Figure 5. The one-pot enzyme-free colorimetric glucose detection based on Au@BSA-GO nanocomposites. a) Schematic of glucose detection strategy. b) The photograph of the reaction solutions containing different concentrations (0–0.5 × 10^{-3} M) of glucose in the presence of Au@BSA-GO nanocomposites. c) The corresponding absorbance spectra. d) Calibration curve for glucose detection.

detection of H_2O_2 were simultaneously performed (**Figure 5**a). For the qualitative assay of glucose, the above strategy was performed with different concentrations of glucose, and the regular changes of blue color in the reaction solutions could be expediently observed by naked eye (Figure 5b). Then, the absorbances of the solution were detected at 650 nm for the quantitative assay of glucose (Figure 5c) and the calibration curve was plotted (Figure 5d). The regression equation was $y = 2.984x + 0.073$ ($R^2 = 0.998$) with the linear range of 0.001–0.3 × 10^{-3} M. The limit of detection was 0.6 μM (S/N = 3), which was lower than that of reported two-step assay[23,32–34] and one-pot enzymatic assay.[35] In addition, the response time (30 min) was shorter than that (more than 7 h) of the reported Au NPs-based enzyme-free assay method.[20] To further testify the reliability, proposed tandem sensing system and glucose meter were used for the detection of glucose (about 5 × 10^{-3} M). The solution of glucose was diluted into the linear range of proposed method and the concentration of glucose was calculated to be 4.09 × 10^{-3} M according to the calibration curve, which was comparable with the result (5.02 × 10^{-3} M) of glucose meter.

Moreover, the storage stabilities of Au@BSA NPs and Au@BSA NPs-GO nanocomposites were studied by the one-pot reaction. After the storage for 30 d at 4 °C, there was not observable reduction for the tandem enzyme-like activity of Au@BSA NPs-GO nanocomposites, and Au@BSA NPs still showed above 95% of the initial activity (Figure S11, Supporting Information), suggesting the excellent storage stabilities of the both catalysts. However, like the previously reported Au catalyst, the both catalysts showed unsatisfactory salt-tolerability (Figure S12, Supporting Information). To research the selectively of Au@BSA NPs-GO nanocomposites, some glucose analogues (fructose, maltose, lactose, sucrose, and galactose) were used as controls. The proposed sensing system based on Au@BSA NPs-GO nanocomposites exhibited poor selectivity (Figure S13, Supporting Information), which is a common challenge for most nanozymes.

Although some studies had showed that Au NPs had GOx-like activities, the two-step strategy was usually used on the glucose detection, because the optimal pH ranges of these GOx mimics were different from those of HRP and peroxidase mimics.[21] In contract, as-synthesized Au@BSA NPs could be used on one-pot glucose assay due to the similar pH ranges of dual enzyme activities. The proposed assay method was enzyme-free, simple, and sensitive. Therefore, the unique tandem nanozyme (Au@BSA NPs) provided a novel avenue for the assay application based on the GOx-like activity of Au NPs.

3. Conclusion

In summary, "non-naked" Au NPs with GOx-like activity are obtained by BSA-directed synthesis and their sizes could be regulated by changing the BSA concentration. Fortunately, "non-naked" Au NPs (Au@BSA NPs) not only have GOx-like activity, but also show the dual activities (peroxidase-like and GOx-like activities) at the same pH. So, as-synthesized Au NPs can be called as "tandem nanozyme." To verify the advantage of the modifiable Au@BSA NPs, GO is used as the model supporter for the covalent modification of Au@BSA NPs. Au@BSA NPs and Au@BSA NPs-GO nanocomposites have similarity activities, indicating that the surface modification of Au@BSA NPs cannot affect their GOx-like activity. Further, Au@BSA NPs-GO

nanocomposites are applied on the fast, one-pot, and nonenzymatic glucose colorimetric detection. The "non-naked" Au not only broadens the species of tandem nanozymes, but also facilitates the functionalization of nanozymes with some molecules, such as antibody, enzyme, and fluorescence probe, which are promising for immunoassay, biosensor, and medical treatment.

4. Experimental Section

Chemicals and Materials: H_2O_2, $HAuCl_4$, and $NaBH_4$ were purchased from Sinopharm Chemical Reagent Co (Shanghai, China). BSA (68 kDa), TMB, ABTS, OPD, lysozyme (EC 3.2.1.17), NHS, GO, and GOx (EC 1.1.3.4) were purchased from Sigma-Aldrich (St. Louis, USA). Sodium citrate and EDC were purchased from Shanghai Ryon Biological Technology Co., Ltd (Shanghai, China). All other reagents were of the analytical grade and used without further purification. The ultrapure water was prepared with Milli-Q system (18.2 MΩ cm).

Apparatus: The morphology analysis was conducted by TEM H-7650 (Hitachi, Japan). Samples for TEM assay were prepared by dropping the diluted Au@BSA NPs solution onto copper grids coated with carbon films and dried at room temperature in air. Zeta potential (ζ) was detected by dynamic light scattering on the Zetasizer Nano ZEN3690 (Malvern Instruments Ltd., Malvern, UK). To obtain XRD pattern of Au@BSA NPs, the materials were dried and analyzed by XRD D8 ADVANCE (Bruker AXS, Germany). The spectrophotometric assay was performed on ultraviolet spectrophotometer TU-1901 (Persee, China). Glucose meter with blood glucose test strips (AGS-1000) was purchased from Andon Health Co., Ltd. (Tianjin, China).

Synthesis of Au@BSA NPs: For the synthesis of Au@BSA NPs, all glassware were cleaned in freshly prepared aqua regia (volume ratio $HCl:HNO_3$ = 3:1) and rinsed thoroughly with water. Then, $HAuCl_4$ aqueous solution (1 mL, 24.3×10^{-3} M) was added into BSA solution (4 mL, 1 μM, 3 μM, 6 μM, 10 μM) under magnetic stirring at room temperature. Afterward, the mixture solution was stirred for 5 min. Then, $NaBH_4$ (100 μL, 1 mg mL^{-1}) was rapidly added into the above mixture. After reaction of 30 min, the Au@BSA NPs were obtained and stored at 4 °C.

Synthesis of Au@lysozyme NPs: Au@lysozyme NPs were obtained by $NaBH_4$ reduction method. First, $HAuCl_4$ aqueous solution (1 mL, 24.3×10^{-3} M) was added into lysozyme solution (4 mL, 0.0034 g, same dosage with BSA in synthesis of Au@BSA NPs) under magnetic stirring at room temperature. Then, the mixture solution was stirred for 5 min. Afterward, $NaBH_4$ (100 μL, 1 mg mL^{-1}) was rapidly added into the above mixture. After reaction of 30 min, the Au@lysozyme NPs were obtained and stored at 4 °C.

*Synthesis of Au@*citrate *NPs*: The Au@citrate NPs were prepared by sodium citrate reduction method. First, $HAuCl_4$ solution (0.4 mL, 24.3×10^{-3} M) was added into 9.6 mL ultrapure water and boiled under magnetic stirring. Then, sodium citrate (1 mL, 38.8×10^{-3} M) was rapidly added to mixture solution under magnetic stirring. After boiling of 30 min, the Au@citrate NPs were obtained and stored at 4 °C.

Peroxidase-Like Activity Characterization: Considering TMB can be oxidized by H_2O_2 to generate colored product (TMB^{*+}) in the presence of the peroxidase mimetics (H_2O_2+TMB→H_2O+TMB^{*+}),[9] TMB was used as a typical substrate to evaluate the catalytic properties of Au@BSA NPs. In a representative test, the reaction system (200 μL) included Au@BSA NPs (3 μg mL^{-1}), TMB (0.5×10^{-3} M), and H_2O_2 (1×10^{-3} M) in acetate buffer (100×10^{-3} M, pH 4.0), and the absorbance was recorded by using the spectrophotometer.

The effect of pH on the catalytic activity of Au@BSA NPs was measured by the above assay, except that the pH (1.0–11.0) of the catalysis reaction system was changed by using different buffers (100×10^{-3} M): glycine-HCl buffer (pH 1.0–2.0), acetate buffer (pH 3.0–5.0), phosphate buffer (pH 6.0–8.0), and Tris-HCl buffer (pH 9.0–11.0). The maximal activity in the experiment was defined as 100% relative activity.

GOx-Like Activity Characterization: The GOx-like activity of Au@BSA NPs was measured by a two-step method. In a representative test, Au@BSA NPs (3 μg mL^{-1}) and glucose (1×10^{-3} M) were incubated in acetate buffer (100×10^{-3} M, pH 4.0). After the reaction (glucose + O_2→H_2O_2 + gluconic acid) for 30 min TMB (0.5×10^{-3} M) and HRP (3 μg mL^{-1}) were added. Then, the absorbance of mixture at 650 nm was recorded.

The effect of pH on the GOx-like activity of Au@BSA NPs was studied by the above assay, except that the pH (1.0–11.0) of the catalysis reaction system was changed. The maximal activity in the experiment was defined as 100% relative activity.

Tandem-Like Activity Characterization: For the tandem enzyme-like activity of Au@BSA NPs, a one-pot reaction was conducted. In a representative test, the reaction solution containing Au@BSA NPs (3 μg mL^{-1}), TMB (0.5×10^{-3} M), and glucose (0.2×10^{-3} M) in acetate buffer (100×10^{-3} M, pH 4.0) was incubated and the absorbance peak of TMB^{*+} was measured at 650 nm.

The impact of pH on the tandem enzyme-like activity of Au@BSA NPs was also researched by the above assay, except that the pH (1.0–11.0) of the catalysis reaction system was changed. The maximal activity in the experiment was defined as 100% relative activity.

Synthesis of Au@BSA NPs-GO Nanocomposites: Au@BSA NPs-GO nanocomposites were synthesized by covalent binding. First, GO (2 mg) was dispersed in 5 mL water and then the carboxyl group of GO was activated by the mixture of EDC (6×10^{-3} M) and NHS (6×10^{-3} M) for 5 h in the dark. Second, the activated GO was incubated with Au@BSA NPs overnight and stored at 4 °C.

Colorimetric Detection of Glucose: For the colorimetric detection of glucose, a one-pot enzyme-free strategy was proposed, based on the tandem enzyme-like activity. The reaction systems containing Au@BSA NPs-GO nanocomposites (equivalently 3 μg mL^{-1} Au@BSA NPs), TMB (0.5×10^{-3} M), and glucose with various concentrations (0–0.8×10^{-3} M) were incubated for 30 min in acetate buffer (100×10^{-3} M, pH 4.0). Then, the above solutions were centrifuged to terminate the reaction, followed by the spectrophotometric assay at 650 nm.

Supporting Information

Supporting Information is available from the Wiley Online Library or from the author.

Acknowledgements

This work was financially supported by the National Natural Science Foundation of China (Grant Nos. 21705087, 21575074, and 21775082), the Special Foundation for Distinguished Taishan Scholar of Shandong Province (Grant No. ts201511052), the Major Basic Research Program of Natural Science Foundation of Shandong Province (Grant No. ZR2018ZC0127), A Project of Shandong Province Higher Educational Science and Technology Program (Grant No. J18KA067), and Research Foundation for Distinguished Scholars of Qingdao Agricultural University (Grant No. 663-1117015).

Conflict of Interest

The authors declare no conflict of interest.

Keywords

biomimetics, biomineralization, glucose oxidase-like activity, nanozymes, tandem catalysis

Received: August 13, 2018
Revised: September 3, 2018
Published online:

[1] Q. Wang, X. Zhang, L. Huang, Z. Zhang, S. Dong, *Angew. Chem., Int. Ed.* **2017**, *56*, 16082.
[2] L. Han, H. Zhang, D. Chen, F. Li, *Adv. Funct. Mater.* **2018**, *28*, 1800018.
[3] Y. Hu, H. Cheng, X. Zhao, J. Wu, F. Muhammad, S. Lin, J. He, L. Zhou, C. Zhang, Y. Deng, P. Wang, Z. Zhou, S. Nie, H. Wei, *ACS Nano* **2017**, *11*, 5558.
[4] H. Wei, E. Wang, *Chem. Soc. Rev.* **2013**, *42*, 6060.
[5] Y. Guo, L. Deng, J. Li, S. Guo, E. Wang, S. Dong, *ACS Nano* **2011**, *5*, 1282.
[6] W. He, X. Wu, J. Liu, X. Hu, K. Zhang, S. Hou, W. Zhou, S. Xie, *Chem. Mater.* **2010**, *22*, 2988.
[7] Z. Chen, J.-J. Yin, Y.-T. Zhou, Y. Zhang, L. Song, M. Song, S. Hu, N. Gu, *ACS Nano* **2012**, *6*, 4001.
[8] R. André, F. Natálio, M. Humanes, J. Leppin, K. Heinze, R. Wever, H.-C. Schröder, W. E. G. Müller, W. Tremel, *Adv. Funct. Mater.* **2011**, *21*, 501.
[9] H. Cheng, L. Zhang, J. He, W. Guo, Z. Zhou, X. Zhang, S. Nie, H. Wei, *Anal. Chem.* **2016**, *88*, 5489.
[10] K. S. Chaturvedi, C. S. Hung, D. E. Giblin, S. Urushidani, A. M. Austin, M. C. Dinauer, J. P. Henderson, *ACS Chem. Biol.* **2014**, *9*, 551.
[11] A. S. Jalilov, L. G. Nilewski, V. Berka, C. Zhang, A. A. Yakovenko, G. Wu, T. A. Kent, A.-L. Tsai, J. M. Tour, *ACS Nano* **2017**, *11*, 2024.
[12] J. Yao, Y. Cheng, M. Zhou, S. Zhao, S. Lin, X. Wang, J. Wu, S. Li, H. Wei, *Chem. Sci.* **2018**, *9*, 2927.
[13] K. Sobańska, P. Pietrzyk, Z. Sojka, *ACS Catal.* **2017**, *7*, 2935.
[14] M. Yamada, N. Yoshinari, N. Kuwamura, T. Saito, S. Okada, S. P. Maddala, K. Harano, E. Nakamura, K. Yamagami, K. Yamanaka, A. Sekiyama, T. Suenobu, Y. Yamada, T. Konno, *Chem. Sci.* **2017**, *8*, 2671.
[15] L. Han, H. Zhang, F. Li, *Part. Part. Syst. Charact.* **2018**, *35*, 1800207.
[16] Y. Lin, J. Ren, X. Qu, *Adv. Mater.* **2014**, *26*, 4200.
[17] M. Comotti, C. Della Pina, R. Matarrese, M. Rossi, *Angew. Chem., Int. Ed.* **2004**, *43*, 5812.
[18] B. Liu, J. Liu, *Nano Res.* **2017**, *10*, 1125.
[19] X. Zheng, Q. Liu, C. Jing, Y. Li, D. Li, W. Luo, Y. Wen, Y. He, Q. Huang, Y. T. Long, C. Fan, *Angew. Chem., Int. Ed.* **2011**, *50*, 11994.
[20] Y. Lin, Z. Li, Z. Chen, J. Ren, X. Qu, *Biomaterials* **2013**, *34*, 2600.
[21] D. Zeng, W. Luo, J. Li, H. Liu, H. Ma, Q. Huang, C. Fan, *Analyst* **2012**, *137*, 4435.
[22] M. Comotti, C. Della Pina, E. Falletta, M. Rossi, *Adv. Synth. Catal.* **2006**, *348*, 313.
[23] L. Han, P. Liu, H. Zhang, F. Li, A. Liu, *Chem. Commun.* **2017**, *53*, 5216.
[24] N. J. Lang, B. Liu, J. Liu, *J. Colloid Interface Sci.* **2014**, *428*, 78.
[25] P. Beltrame, M. Comotti, C. Della Pina, M. Rossi, *Appl. Catal., A* **2006**, *297*, 1.
[26] S. C. Smith Jr., *Am. J. Med.* **2007**, *120*, S3.
[27] W. Luo, Y.-S. Li, J. Yuan, L. Zhu, Z. Liu, H. Tang, S. Liu, *Talanta* **2010**, *81*, 901.
[28] W.-I. Kanchana, T. Sakai, N. Teshima, S. Katoh, K. Grudpan, *Anal. Chim. Acta* **2007**, *604*, 139.
[29] R. N. Ammeraal, G. A. Delgado, F. L. Tenbarge, R. B. Friedman, *Carbohydr. Res.* **1991**, *215*, 179.
[30] Y. Bai, Y. Sun, C. Sun, *Biosens. Bioelectron.* **2008**, *24*, 579.
[31] W. Chen, J. Chen, Y.-B. Feng, L. Hong, Q.-Y. Chen, L.-F. Wu, X.-H. Lin, X.-H. Xia, *Analyst* **2012**, *137*, 1706.
[32] Y. Jv, B. Li, R. Cao, *Chem. Commun.* **2010**, *46*, 8017.
[33] L. Han, L. Zeng, M. Wei, C. M. Li, A. Liu, *Nanoscale* **2015**, *7*, 11678.
[34] C. Xia, X. Hai, S. Chen, X. W. Chen, J. H. Wang, *Chin. J. Anal. Chem.* **2016**, *44*, 41.
[35] L. Han, C. Li, T. Zhang, Q. Lang, A. Liu, *ACS Appl. Mater. Interfaces* **2015**, *7*, 14463.